

Optical Responses of Negative-Copper-Ion Implanted Al₂O₃

Oleg A. Plaksin^{1,2}, Yoshihiko Takeda¹, Hiroshi Amekura¹, Kenichiro Kono¹
Naoki Umeda³ and Naoki Kishimoto¹

¹Nanomaterials Laboratory, National Institute for Materials Science, Tsukuba, Ibaraki 305-0003, Japan
Fax: 81-298-59-5010, e-mail: plax@mail.ru

²State Scientific Centre of Russia Federation – Institute of Physics and Power Engineering, Obninsk, 249033, Russia

³University of Tsukuba, Tsukuba, Ibaraki 305-8573, Japan

To monitor formation of Cu nanoparticles, spectra of the optical transmission of Al₂O₃ were measured during implantation of 60 keV Cu⁻ ions at ion fluxes from 5 to 50 μA/cm². The precipitation threshold is flux-dependent and occurs at the lower ion fluences for the higher ion fluxes. The formation of nanoparticles is (a) efficient up to a fluences of 2×10¹⁷ ions/cm² or more and (b) most efficient for a flux of 50 μA/cm². Intrinsic size effects have little influence on the linear and non-linear optical absorption of nanocomposites.

Key words: ion implantation, metal nanoparticles, insulators, optical absorption, non-linear optical response

1. INTRODUCTION

Metal nanoparticles embedded in transparent insulators are promising for optical devices, since surface-plasmon resonance (SPR) causes ultra-fast non-linear response [1-2]. Having an advantage to inject immiscible elements, the heavy-ion implantation of insulators became an efficient method of fabrication of the two-dimensional metal-nanoparticle composites. Fabrication of nanocomposites is controlled rather well via variation of the ion energy, flux and fluence, and furthermore, the number of atoms in metal nanoparticles can be monitored by means of *in-situ* measurements of optical absorption in the range of the surface-plasmon-resonance (SPR) peak [3-4].

Although the high-flux implantation is very attractive to shorten the fabrication time, the ion fluxes allowable for efficient formation of nanocomposites are limited, for example, to about 10 μA/cm² for silica glasses (a-SiO₂) or 1 μA/cm² for LiNbO₃, etc [4-5]. Moreover, implantation of 60 keV Cu⁻ ions into LiNbO₃ resulted in (a) the change of chemical composition and structure of implanted regions of LiNbO₃ and (b) formation of complex nanocomposites consisting of metal Cu nanoparticles distributed among nanodomains of the host medium with variable composition. The chemical composition change and its spatial modulations caused the ion-flux-dependent variations of linear (Fig.1) and non-linear optical absorption of the nanocomposites.

Another important issue for ion implantation is stability of nanocomposites under ion bombardment. Saturation behaviors of optical absorption in the range of SPR of a-SiO₂ and LiNbO₃ observed at high ion fluxes were tentatively related to the preferential energy deposition to Cu nanoparticles [4-5], though other flux-dependent processes should be taken into account (radiation-enhanced diffusion, heating, sputtering, etc.).

In the present study, we challenged the high-flux implantation of sapphire (Al₂O₃), one of the most radiation-resistant optical materials [6-7]. We conducted measurements of optical transmission during implantation of negative 60 keV Cu ions into Al₂O₃ at

various ion fluxes with the purpose to observe and study the formation of Cu nanoparticles. For as-fabricated nanocomposites, the non-linear optical responses were measured. In this paper, we will discuss the *in-situ* optical measurements and the non-linear optical techniques in fabrication and characterization of nanocomposites respectively.

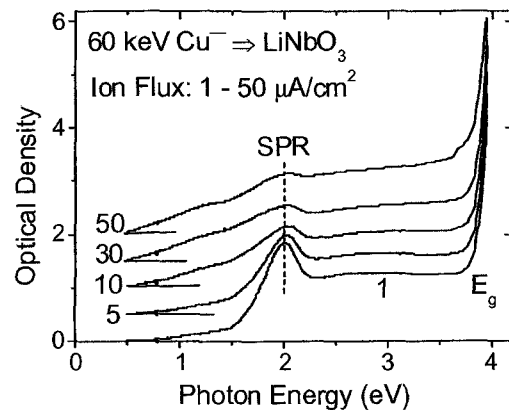


Fig.1. Spectra of optical absorption of LiNbO₃ measured *ex-situ* after implantation by 60 keV Cu⁻ ions to the same fluence of 2×10¹⁷ ions/cm² at various ion fluxes.

2. EXPERIMENTAL

Disk-shaped specimens of Al₂O₃ single crystals (∅15 mm × 0.5 mm) polished to optical grade were irradiated by 60 keV Cu⁻ ions at various ion fluxes from 5 to 50 μA/cm² (3×10¹³ – 3×10¹⁴ ions/cm²s) up to a fluence of 2×10¹⁷ ions/cm². The beam current was measured before and after ion implantation, with the help of a Faraday cup of 40 mm in diameter. To reduce the heat loads, the specimens were placed in a massive sample holder made of copper and covered by a copper mask with a hole of 12 mm in diameter. With the same purpose, the beam cross-section was shaped into 12 mm diameter circle through an aperture, and the beam was aligned onto the same area of the substrate surface. The

Xe lamp illuminated the back surfaces of the specimens through a hole in the sample holder (Fig.2), at an angle of incidence of 35° to the beam direction. Intensified CCD cameras collected spectra of optical transmission T in the range of photon energies from 1.7 to 2.7 eV. The optical loss (OL) was calculated using the formula

$$OL = -\ln(T). \quad (1)$$

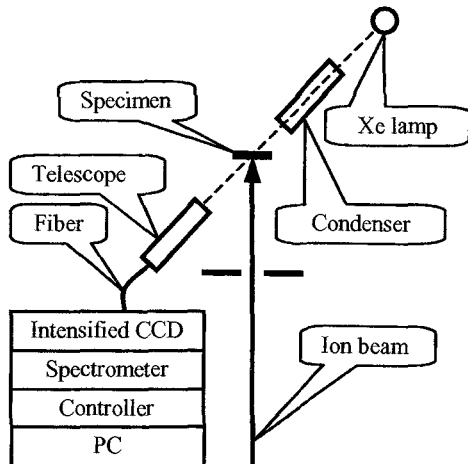


Fig.2. Schematic diagram of experiment

To calculate the absorption we also measured *ex-situ* the optical transmission and reflection of as-implanted specimens, by using a dual beam spectrometer. Optical density (αL , with α and L , the absorption coefficient and the thickness of nanocomposite respectively) was calculated using the method described in [8]. Peaks typical for SPR at 2 eV in the absorption spectra indicated the formation of Cu nanoparticles (Fig.3).

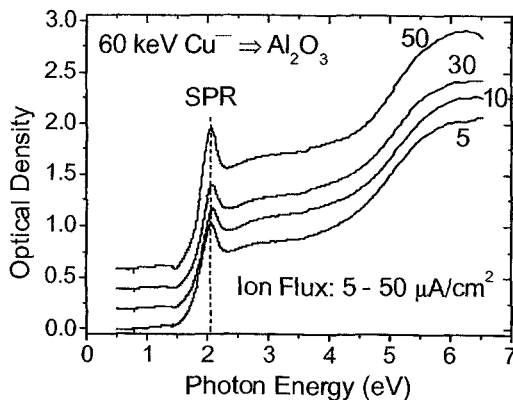


Fig.3. Spectra of optical absorption of Al_2O_3 measured *ex-situ* after implantation by 60 keV Cu^- ions to the same fluence of 2×10^{17} ions/ cm^2 at various ion fluxes.

Negative non-linear optical absorption ($\Delta\alpha < 0$, transient bleaching) was measured by using the Z-scan method [9] with a laser pulse of < 200 fs, repetition rate of 1 kHz, photon energy from 1.9 to 2.5 eV and intensity up to 200 GW/cm^2 at the laser beam waist. Irreversible change of non-linear optical properties was observed at intensities higher than about 500 GW/cm^2 . Distribution of Cu implants was estimated with the TRIM code [10]. The mean projected range R_p of 60 keV Cu^- ions for Al_2O_3 is 29 nm and the straggling is 10 nm. Sputtering

yields were calculated with the TRIDYN code [11] that takes into account the change of chemical composition of substrates with the fluence of ion irradiation.

3. RESULTS AND DISCUSSION

The SPR peak of as-implanted samples (Fig.3) is more pronounced as compared to that of nanocomposites fabricated in a- SiO_2 or LiNbO_3 at the same conditions, but, for magnesium spinel [12], its height is almost the same. Unlike LiNbO_3 , the shape of SPR peak for Al_2O_3 does not change with an ion flux. The position and shape of SPR peak for Al_2O_3 are almost the same as that predicted by the Maxwell-Garnet approximation [13] or Mie theory, according to the formula

$$\alpha = \frac{9p\varepsilon_d}{k} \frac{\varepsilon_2}{(\varepsilon_1 + 2\varepsilon_d)^2 + \varepsilon_2^2}, \quad (2)$$

where p is the volume fraction of nanoparticles, ε_d is the dielectric constant of matrix, k is the wave vector, ε_1 and ε_2 are the real and imaginary parts of dielectric function of bulk metal respectively. In general, it is evident that the efficiency of Cu nanoparticle formation in Al_2O_3 is flux-dependent: it is most efficient for 50 $\mu\text{A}/\text{cm}^2$. However, the optical absorption measured *in-situ* usually reveals more details [4-5].

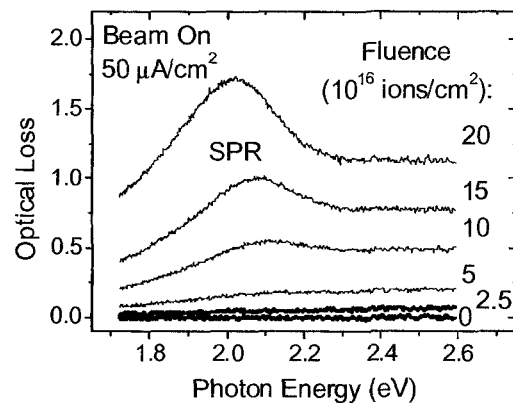


Fig.4. Spectra of optical absorption of Al_2O_3 measured *in-situ* at an ion flux of 50 $\mu\text{A}/\text{cm}^2$.

As monitored *in-situ*, the SPR peak slightly shifts to lower photon energies (red-shift) with increasing the fluence (Fig.4). The shift of SPR with increasing the fluence is almost the same when measured for various ion fluxes. As known [3], spectra of optical absorption measured *in-situ* may differ from those measured *ex-situ*, for example, because of contributions from the absorption bands observed solely under irradiation (transient absorption). To separate transient absorption, we monitored SPR peak within several minutes after the ion beam was switched off. No transient absorption was observed. Therefore, the optical absorption measured *in-situ* at the photon energy of SPR should be roughly proportional to the number of Cu atoms in nanoparticles, though various intrinsic and extrinsic effects of the nanoparticle size might contribute to the absorption [14]. It is noteworthy that the pill-out effect or the classical damping of electron motion, which are most often discussed in the context of optical response of nanoparticles [14], have to cause a red-shift of SPR with

increasing the nanoparticle diameter (say increasing the ion fluence).

Fluence dependencies of optical loss at SPR measured at various ion fluxes are shown in Fig.5, where the difference between irradiated and un-implanted states of a sample is presented. The precipitation threshold, determined as the fluence, at which the SPR peak appears, decreases from 2.5×10^{16} to 1×10^{16} ions/cm² with increasing the ion flux from 5 to 50 $\mu\text{A}/\text{cm}^2$. Further increase of the SPR peak with the fluence is not linear. The increasing slope of the fluence dependencies suggests that nanoparticle formation is efficient at fluences of more than 2×10^{17} ions/cm².

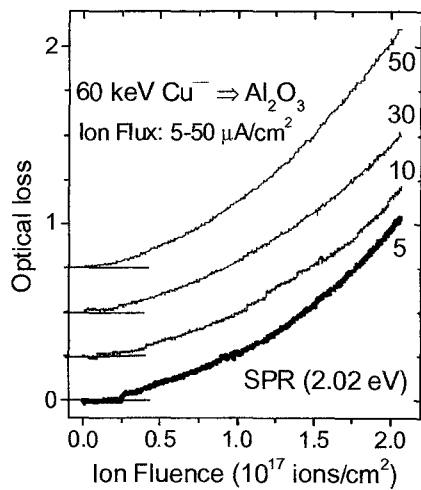


Fig.5. Fluence dependencies of optical absorption at the energy of SPR (2.02 eV) taken for various ion fluxes.

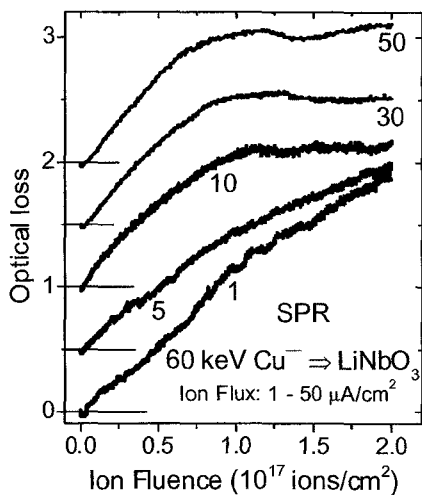


Fig.6. Fluence dependencies of (a) absorbance at the energy of SPR (2 eV) taken for various ion fluxes.

The absorption at the SPR increases gradually up to an ion fluence of 2×10^{17} ions/cm², even at high ion fluxes, unlike that for a-SiO₂ and LiNbO₃ (Fig.6), for which saturation behavior at above 1×10^{17} ions/cm² was observed if the ion fluxes were higher than 10 $\mu\text{A}/\text{cm}^2$ [4-5]. As shown in those papers, the saturation at high fluxes is evidence that nanoparticles are frequently destroyed by Cu ion bombardment. The destruction of

Cu nanoparticles in a-SiO₂ or LiNbO₃ may be enhanced because of the preferential deposition of ion energy into nanoparticles, which was confirmed by TRIM calculations for metal Cu layers embedded into a-SiO₂ or LiNbO₃ (Fig.7). The TRIM calculations predict that more than 90% of energy of 60 keV Cu⁻ ions is spent for recoil production in a-SiO₂, LiNbO₃, Al₂O₃ or metal copper. As shown in Fig.7, the energy deposited to the metal layer of 10 nm of thickness, located in a-SiO₂ or LiNbO₃ matrix at a depth of 20 nm, is significantly larger than that deposited to the matrix. The results shown in Fig.7 must be considered as a possible tendency since some of important features are not taken into account in TRIM calculations. Firstly, ion-energy losses in nanoparticles may differ from that in metal layers. Secondly, nanoparticles are surrounded by a solid solution with the Cu concentration depending on the depth, but not a pure oxide. As is also, the channeling effects that may take place in crystalline materials are not taken into account by the TRIM code. The idea that the structures of metal nanocomposites may depend on the gradients of ion-energy loss between the media and nanoparticles must be implemented in a more sophisticated model.

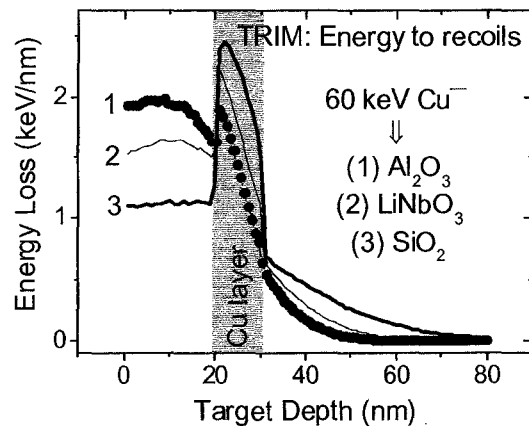


Fig.7. Depth distributions of energy loss of 60 keV Cu⁻ ions in targets consisting of Cu layers embedded into substrates of a-SiO₂, LiNbO₃ or Al₂O₃.

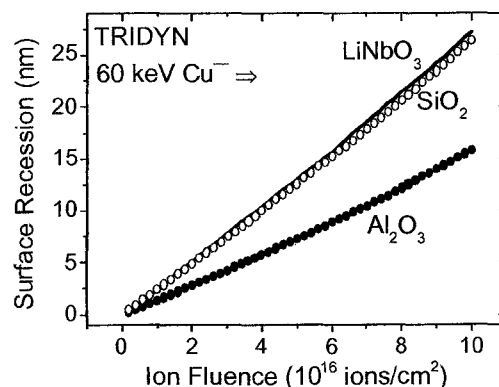


Fig.8. Surface recession of Al₂O₃, SiO₂ and LiNbO₃ under 60 keV Cu⁻ ion implantation.

Destruction of nanoparticles in Al₂O₃ may become an important factor at fluxes higher than 50 $\mu\text{A}/\text{cm}^2$, or at

fluences higher than 2×10^{17} ions/cm². In sapphire, Cu nanoparticles must be more stable since there is probably no preferential energy deposition into the metal Cu phase, as shown by TRIM calculations for Cu layers. Another reason of the saturation behavior shown in Fig.6 may be the competition between accumulation of implants, diffusion and surface recession (the latter is due to sputtering). Substrates of Al_2O_3 must not so suffer from sputtering as a- SiO_2 or LiNbO_3 , as predicted by TRIDYN calculations (Fig.8). In particular, sputtering yields (in atoms/ion) for Al_2O_3 and SiO_2 are almost the same, but the latter has as twice as smaller the atom number density, which causes a larger surface recession (S_r). However, the projected range of ions R_p is larger for smaller density of substance. If diffusion is not considered, the ratio R_p/S_r can be taken as a criterion related to the ion fluence necessary for saturation. The ratio is almost the same for Al_2O_3 and SiO_2 , though it is as twice as smaller for LiNbO_3 . It suggests that diffusion coefficient or other properties must be included into the criterion. It should be noted that post-collision processes such as diffusion are not considered in TRIDYN or TRIM calculations. Criteria related to the saturation behavior will be discussed in forthcoming papers.

In many cases, linear and non-linear optical absorption of the metal-nanoparticle composites fabricated at various conditions of implantation correlate with each other ($\Delta\alpha/\alpha \approx \text{const}$) [15]. Theoretically, in dilute composites, both of them must be proportional to the volume fraction of nanoparticles [15]. To study correlations between linear and non-linear optical absorption, non-linear optical responses of as-implanted samples were measured by the Z-scan method. Difference between the maximum and minimum values of optical transmission ($\Delta T/T \sim -\Delta\alpha L$) at the Z-scan profiles is shown in Fig.9. The flux-dependence of the non-linear optical absorption is mainly caused by difference in linear optical absorption of nanocomposites. When normalized by an optical density αL , the non-linear optical response ($\Delta T/T\alpha L \sim -\Delta\alpha/\alpha$, closed circles in Fig.9) is almost independent of the ion flux. The slight variation of $\Delta\alpha/\alpha$ may be caused by a change of contributions of intraband and interband transitions in metal Cu nanoparticles via intrinsic size effects.

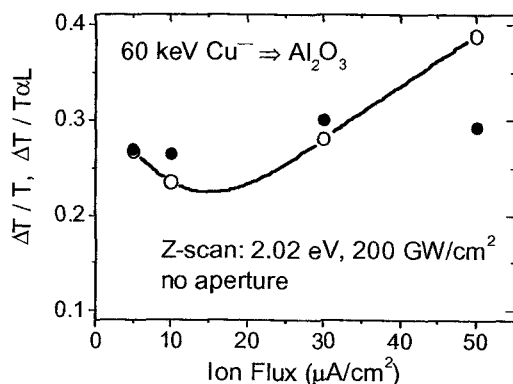


Fig.9. Ion-flux dependencies of the amplitude $\Delta T/T$ of Z-scan profile measured with no aperture (open circles) and the amplitude $\Delta T/T$ normalized by the optical density of corresponding as-implanted samples (closed circles). The solid line is given for reference.

4. CONCLUSION

Spectra of the optical transmission of Al_2O_3 were measured during implantation of 60 keV Cu^- ions at ion fluxes from 5 to 50 $\mu\text{A}/\text{cm}^2$ up to a fluence of 2×10^{17} ions/cm². The optical transmission in the range of SPR is a reliable monitor of nanocomposite formation. The precipitation threshold of Cu atoms is flux-dependent. The formation of nanoparticles is (a) efficient up to a fluence of 2×10^{17} ions/cm² and (b) most efficient at an ion flux of 50 $\mu\text{A}/\text{cm}^2$. Correspondingly, the strongest non-linear optical response $\Delta\alpha$ is observed for 50 $\mu\text{A}/\text{cm}^2$. The non-linear optical response is roughly proportional to a number of Cu atoms in nanoparticles. Intrinsic size effects do not dominate the linear and non-linear optical absorption of as-implanted Al_2O_3 .

ACKNOWLEDGEMENT

A part of this study was financially supported by the Budget for Nuclear Research of the MEXT, based on the screening and counseling by the Atomic Energy Commission.

REFERENCES

- [1] R. F. Haglund, *Materials Science and Engineering A*, **253**, 275-283 (1998).
- [2] Y. Takeda, C.G. Lee, N. Kishimoto, *Nuclear Instruments and Methods B*, **191**, 422-427 (2002).
- [3] O.A. Plaksin, N. Okubo, Y. Takeda, H. Amekura, K. Kono, N. Kishimoto, *Nuclear Instruments and Methods B*, **219-220**, 294-298 (2004).
- [4] O.A. Plaksin, Y. Takeda, H. Amekura, N. Umeda, K. Kono, N. Okubo, N. Kishimoto, *Applied Surface Science*, **244**, 79-83 (2005).
- [5] O.A. Plaksin, Y. Takeda, K. Kono, H. Amekura, N. Umeda, N. Kishimoto, *Applied Surface Science*, **241**, 213-217 (2005).
- [6] A. L. Stepanov, U. Kreibig, D. E. Hole, R. I. Khaibullin, I. B. Khaibullin, V. N. Popok, *Nuclear Instruments and Methods B*, **178**, 120-125 (2001).
- [7] M. Ikeyama, S. Nakao, M. Tazawa, K. Kadono, K. Kamada, *Nuclear Instruments and Methods B*, **175-177**, 652-657 (2001).
- [8] H. Amekura, Y. Takeda, H. Kitazawa, N. Kishimoto, *Proceedings of SPIE*, **4977**, 639-647 (2003).
- [9] Y. Takeda, J. Lu, O. A. Plaksin, H. Amekura, K. Kono, N. Kishimoto, *Nuclear Instruments and Methods B*, **219-220**, 737-741 (2004).
- [10] Ziegler J.F., Biersack J.P., "The Stopping and Ion Range in Solids", Pergamon Press, New York (1985).
- [11] TRIDYN Vs. 4.0 by W. Möller and W. Eckstein, Department of Surface Physics, Max-Planck Institute of Plasma Physics, Garching, Germany (1989).
- [12] V. Bandourko, T. T. Lay, Y. Takeda, C.G. Lee, N. Kishimoto, *Nuclear Instruments and Methods B*, **175-177**, 68-73 (2001).
- [13] J.C. Maxwell-Garnett, *Philosophical Royal Society, London*, **205**, 237-288 (1906)
- [14] U. Kreibig, M. Volmer, "Optical Properties of Metal Clusters", Springer-Verlag, Berlin, 1995.
- [15] K. Uchida, S. Kaneko, S. Omi, C. Hata, H. Tanji, Y. Asahara, A. J. Ikushima, *Journal of Optical Society of America B*, **11**, 1236-1243 (1994).